


# Intrabeam Radiation Inhibits Proliferation, Migration, and Invasiveness and Promotes Apoptosis of MCF-7 Breast Cancer Cells

Technology in Cancer Research & Treatment  
Volume 18: 1-7  
© The Author(s) 2019  
Article reuse guidelines:  
sagepub.com/journals-permissions  
DOI: 10.1177/1533033819840706  
journals.sagepub.com/home/tct  


Lingxiao Pan, MD<sup>1,2</sup>, Minghui Wan, MD<sup>3</sup>, Wenbo Zheng, MD<sup>2</sup>, Rui Wu, MD<sup>4</sup>, Wei Tang, PhD<sup>2</sup>, Xiaoshen Zhang, MD<sup>2</sup>, Tong Yang, MD<sup>5</sup>, and Changsheng Ye, MD<sup>1</sup>

## Abstract

Intraoperative radiotherapy differs from the more commonly used external beam radiation with respect to fractionation, radiation energy, dose rate, and target volume, which may influence the irradiated cells in a complex manner. However, experimental studies of intraoperative radiotherapy are limited. Intrabeam is a frequently used intraoperative radiotherapy device; we evaluated its effects on the proliferation, apoptosis, migration, and invasion of MCF-7 human breast cancer cells. We performed colony formation assays for cells irradiated with single radiation doses of 0 to 16 Gy. Other cells were irradiated with single radiation doses of 0 to 6 Gy and then continued to be cultured. We measured cell-cycle distributions and apoptosis rates 24 hours later, using flow cytometry, and performed wound-healing assays, Transwell tests, and terminal deoxynucleotidyl transferase-mediated 2'-deoxyuridine 5'-triphosphate nick-end labeling staining 4 weeks later. Colony formation assays showed no positive colonies from cells irradiated with doses of  $\geq 6$  Gy. In flow cytometry, the experimental groups had higher late-apoptosis/necrosis rates ( $P < .01$ ) and higher percentages of cells arrested in G<sub>1</sub> phase ( $P < .01$ ). Experimental groups also had much lower scratch-repair rates in the wound healing assay ( $P < .001$ ) and higher apoptosis rates in the terminal deoxynucleotidyl transferase-mediated 2'-deoxyuridine 5'-triphosphate nick-end labeling assay ( $P < .05$ ). In Transwell tests, the 4 Gy and 6 Gy groups had fewer invading cells than the control group ( $P < .05$ ). Single-dose irradiation of 6 Gy with the Intrabeam device can effectively inhibit proliferation, migration, and invasiveness and promote apoptosis in MCF-7 cells with long-lasting effects.

## Keywords

breast cancer, irradiation, proliferation, migration, invasion, apoptosis

## Abbreviations

ANOVA, analysis of variance; DMEM, Dulbecco's Modified Eagle Medium; EBRT, external beam radiotherapy; FBS, fetal bovine serum; IORT, intraoperative radiotherapy; PBS, phosphate-buffered saline; PE, plating efficiency; PI, propidium iodide; SF, surviving fraction; TUNEL, terminal deoxynucleotidyl transferase-mediated 2'-deoxyuridine 5'-triphosphate nick-end labeling

Received: September 06, 2018; Revised: December 08, 2018; Accepted: February 25, 2019.

## Introduction

Breast cancer is a common malignancy in women. The American Cancer Society estimates that approximately 266 000 new breast cancer diagnoses and 40 000 deaths from breast cancer will occur in the United States in 2018.<sup>1</sup> Radiotherapy is widely used as local treatment for breast cancer, and radiotherapy modalities for breast cancer include external beam radiotherapy (EBRT), brachytherapy, and intraoperative radiotherapy (IORT). In contrast to EBRT and brachytherapy, IORT only uses a single large irradiation dose. Because the effective radiation target area of IORT is small and the dose attenuation is rapid, the effect on nonirradiated areas are minimized.<sup>2,3</sup>

<sup>1</sup> Breast Center, Nanfang Hospital, Southern Medical University, Guangzhou, China

<sup>2</sup> Department of Breast Surgery, the First Affiliated Hospital of Guangzhou Medical University, Guangzhou, China

<sup>3</sup> Department of Radiation Oncology, the First Affiliated Hospital of Guangzhou Medical University, Guangzhou, China

<sup>4</sup> Department of Radiotherapy, the First Affiliated Hospital of Guangzhou Medical University, Guangzhou, China

<sup>5</sup> Department of Pathology, the Second Affiliated Hospital (Panyu branch) of Guangzhou Medical University, Guangzhou, China

## Corresponding Author:

Changsheng Ye, MD, Breast Center, Nanfang Hospital, Southern Medical University, No.1838, Guangzhoudadao Street, Baiyun District, Guangzhou 510515, China.

Email: yech\_sh2006@163.com



The species and other characteristics of radioactive rays vary in different IORT equipment. Intrabeam (Carl Zeiss, Oberkochen, Germany) is a small, mobile IORT device with adjustable source applicator direction. Its low-energy X-ray (50 kV) can generate high-ionization density radiation for local radiotherapy, and the spatial irradiation dose attenuates rapidly.<sup>4</sup> Intrabeam was first and most widely used in breast-conserving surgery. It is also used for gastrointestinal cancer, brain cancer, skin cancer, spinal metastasis, and head and neck cancer.<sup>2,5-9</sup>

Experimental researches on IORT remains limited. Belletti *et al*<sup>10</sup> found that postoperative drainage liquid could promote the proliferation, migration, and invasion of breast cancer cells, but these effects were almost completely abrogated in drainage fluid from patients who received IORT. Wound drainage fluid from IORT patients could alter the expression of several cytokines and failed to properly stimulate the activation of some intracellular signal transduction pathways. Some colony formation experiments<sup>11-13</sup> have shown that under the same irradiation dose rates, decreased photon energy will decrease cell survival rates, with survival curves showing decreasing survival tendency with increasing radiation dose. The relative biological effectiveness of Intrabeam IORT is higher than that of the commonly used EBRT. In this study, we explored cytological changes in the human breast cancer cell line MCF-7 at the early and late stages after single irradiation treatments with the Intrabeam device.

## Materials and Methods

### Cell Culture

Human breast cancer MCF-7 cells (Breast Tumor Centre of SunYat-Sen Memorial Hospital, Guangzhou, China) were grown in 10% fetal bovine serum (FBS; Gibco, Thermo Fisher, Waltham, Massachusetts) and 90% Dulbecco's Modified Eagle Medium (DMEM, Gibco), at 37°C in an atmosphere containing 5% CO<sub>2</sub>. The culture medium was free of insulin and was changed every 2 or 3 days. The cells were subcultured in trypsin EDTA solution (Gibco). Prior to the experiments, the cells were subcultured approximately 5 to 10 times in our laboratory.

### Radiation Device and Radiation Parameter Setting

Flat application of the Intrabeam device (PRS 500; Carl Zeiss) could decrease radiation doses according to flat distance. To ensure all cells received uniform radiation doses, flat applicators of 60-mm diameter and T-25 cell culture flasks (Thermo Fisher Scientific) were used in this study. When applying radiation, the flat applicator was placed upside down and the cell culture flask was placed on the surface of applicator, making the bottom of the flask overlay with the surface of applicator to the extent possible. The plastic-shell thickness at the bottom of the flask was 1.2 mm (measured by a Vernier caliper); the density of the plastic was close to human tissue density and the MCF-7 cells were grown in monolayers in the culture

medium. Thus, the target depth was set as 1.2 mm from the flat applicator surface. Before the experiment, the transformation output factor between bare source and target radiation dose (at the adherent cell site) was measured using a water tank with an ionization chamber. The calculated result was 1.31, and the corresponding target radiation dose rate was 14.8 Gy/h.

### Colony Formation Assay

A total of 1000 cells were seeded separately in each flask (T-25) and radiation with 50 kV X-rays from the Intrabeam were administered approximately 4 hours after the cells were seeded. At this time, cells were attached to the bottom of flask but had not divided. For the experimental groups, the single radiation doses were 2 Gy, 4 Gy, 6 Gy, 8 Gy, 12 Gy, or 16 Gy. Cells were further incubated for 12 days, with medium changed only on day 7. The colonies were then fixed with methanol (15 minutes) and stained with 0.5% crystal violet (15 minutes). Colonies (>50 cells) were scored under the microscope. Each experiment was repeated 3 times. Surviving fraction (SF) was calculated as follows: SF = [average number of colonies per flask in the irradiated group/average number of colonies per flask in the control group × 100%]. Plating efficiency (PE) was calculated as follows: PE = [average number of colonies per flask in the control group/number of seeded cells per flask × 100%].

### Cell Preparations for the Following Experiments

The medium was changed when the cells had reached approximately 70% confluency in the T-25 flask, and the cells were then subjected them to radiation approximately 12 hours later. For the experimental groups, the single radiation doses were 2 Gy, 4 Gy, or 6 Gy. Three independent repeat experiments were performed for each experimental group and the control group. Some cells were incubated for another 24 hours and then were harvested for flow cytometry. The other cells were cultured and subcultured for about 4 weeks and were then harvested for wound healing assays, Transwell assays, and terminal deoxynucleotidyl transferase mediated 2'-deoxyuridine 5'-triphosphate nick-end labeling (TUNEL) staining.

### Flow Cytometry for Cell Apoptosis and Cell Cycle

For apoptosis detection,  $1 \times 10^6$  cells in 100  $\mu$ L stain buffer were added with 5  $\mu$ L Annexin V-FITC (BD Pharmingen, San Diego, California) and 5  $\mu$ L propidium iodide (PI; BD Pharmingen, San Diego, California). After incubation for 15 minutes away from light, the cells were evaluated by flow cytometry.

For cell-cycle detection,  $1 \times 10^5$  cells in 100  $\mu$ L phosphate-buffered saline (PBS) were fixed in 75% ethanol at -20°C overnight. The cells were centrifuged, washed with PBS twice, and then incubated in 100  $\mu$ L PBS containing RNase A (1 mg/mL, Sigma, St. Louis, Missouri) for 30 minutes at room temperature.

Finally, the samples were stained with 0.5 mL PI (50  $\mu\text{g/mL}$ ) for 30 minutes away from light at room temperature, followed by detection by flow cytometry.

### Wound Healing Assay

We seeded MCF-7 cells in 12-well plates ( $5 \times 10^4$  cells per well) and incubated them for 24 hours. Scratches were introduced into the monolayers of confluent adherent cells in each well using a sterile pipette tip. Cells were washed twice with PBS and were then incubated in serum-free medium. Images were taken by microscopy (Olympus, Tokyo, Japan) 48 and 72 hours later. Wound areas were observed and calculated using the software tool ImageJ (version 1.51). Average scratch widths for each sample were analyzed. Scratch repair rate (%) = [(original scratch width – scratch width at 48 [or 72] hours)/original scratch width  $\times 100\%$ ].

### Transwell Assay

We plated MCF-7 cells in serum-free media on the inserts of a Corning BioCoat Matrigel Invasion Chamber ( $1 \times 10^5$  cells/well; Corning, Tewksbury, Massachusetts) in 24-well plates. Medium containing 20% FBS plus 80% DMEM was added to the lower chamber. After a 16-hour incubation, invasive cells were fixed with 4% paraformaldehyde at 4°C for 10 minutes and stained with 0.1% crystal violet for 20 minutes. Cells on the upper surface of the membrane were removed with a cotton swab and air-dried. We took images at  $\times 100$  magnification from each membrane and counted the invasive cells.

### TUNEL Staining for Apoptosis Assessment

Following washing of MCF-7 cells in PBS, cells were fixed in 4% paraformaldehyde for 25 minutes and then treated with 0.2% Triton X-100 solution for 5 minutes. We assessed apoptosis using TUNEL (DeadEnd Fluorometric TUNEL System, Promega, Madison, Wisconsin) according to the manufacturer's instructions. Samples were then evaluated under a fluorescence microscope (DMI 6000 B; Leica, Stuttgart, Germany) at  $\times 100$  magnification, and percentages of TUNEL-positive cells were calculated.

### Statistical Analysis

Normally distributed data are shown as mean  $\pm$  standard deviation. We used SPSS version 19.0 software (IBM Corp, Armonk, New York) to perform statistical analysis. Statistical comparisons were made using 1-way analysis of variance (ANOVA). Value of  $P < .05$  was considered significant. The multitarget click model of GraphPad Prism 5.0 (Systat Software, Inc, San Jose, California) was used to generate the cell survival curve.

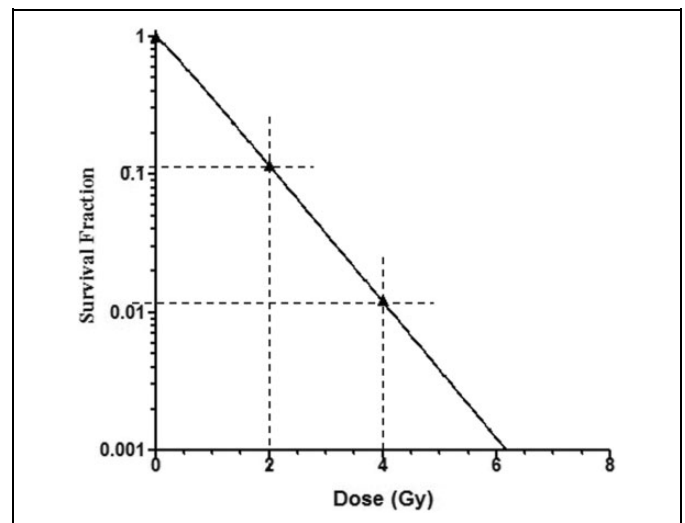


**Figure 1.** Cell survival curve for MCF-7 cells irradiated by the Intrabeam device (50 kV X-ray source) with a flat applicator. Adherent cells in T-25 flasks were irradiated at a constant dose rate of 14.8 Gy/h. Results show the mean of 3 independent experiments.

## Results

### Single-Dose Irradiation With the Intrabeam Inhibited Cell Proliferation

Colony formation assays indicated that the MCF-7 cells in the control group were in logarithmic division, with colony-like distribution. In the experimental groups (especially those that had received doses of  $\geq 6$  Gy), cell proliferation became much slower, most of the cells swelled, fewer mitotic cells were seen, and cell communities were unevenly distributed. In the control samples, the average number of positive clones was 246 (PE = 24.6%). As the radiation dose increased, the numbers of positive clones greatly decreased; no positive clone was found in the groups with doses of  $\geq 6$  Gy. The cell survival curve fitted by positive clone numbers is shown in Figure 1.

### Single-Dose Irradiation With the Intrabeam Induced Apoptosis/Necrosis and $G_1$ Phase Arrest at 24 Hours After Treatment

MCF-7 apoptosis was detected by Annexin V-FITC/PI staining (Figure 2A and B). One-way ANOVA indicated that the late apoptosis/necrosis ratios were greater in the 2 Gy ( $P = .003$ ), 4 Gy ( $P < .001$ ), and 6 Gy ( $P = .001$ ) groups than in the control group. The negative rates in the 4 Gy ( $P = .003$ ) and 6 Gy ( $P = .037$ ) groups were significantly lower than in the control group. However, there were no significant differences in the early apoptosis ratios between the experimental and control groups ( $P > .05$ ).

The flow cytometry results for cell-cycle distribution are shown in Figure 2C and D. Greater numbers of cells were stagnated in  $G_1$  phase in each experimental group compared with the control group (all  $P$  values were  $< .01$ ).

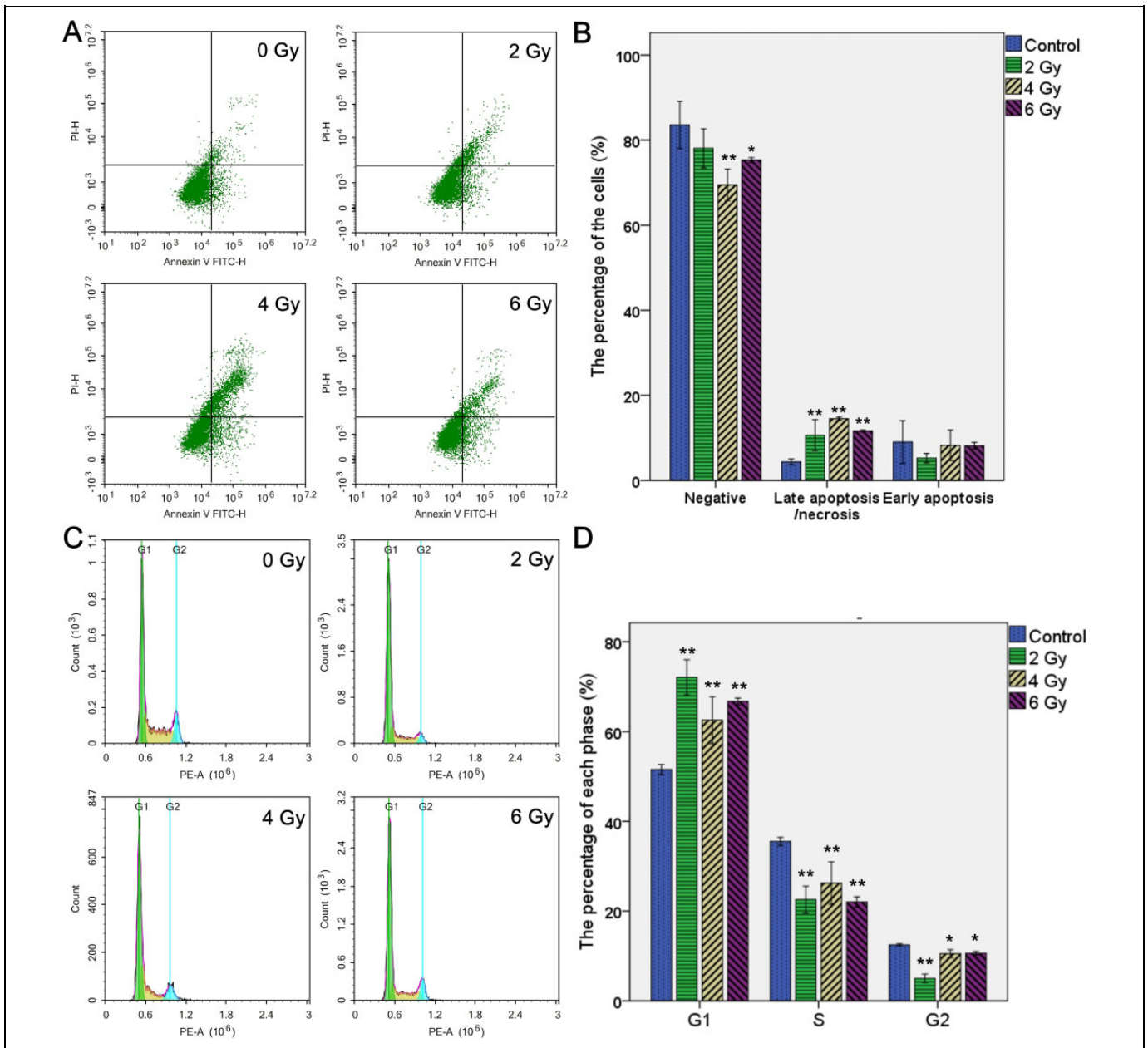


**Figure 2.** Flow cytometry Annexin V-FITC/PI apoptosis analyses and cell-cycle analyses of MCF-7 cells 24 hours after single-dose irradiation with the Intrabeam device. A, Intact viable cells (lower left), early apoptotic cells (lower right), and late apoptotic or necrotic cells (upper right). B and D, Data are expressed as mean  $\pm$  SD; \* $P < .05$ , \*\* $P < .01$  (vs control group); results show the mean of 3 independent experiments. PI indicates propidium iodide; SD, standard deviation.

### Single-Dose Irradiation With the Intrabeam Inhibited Migration and Invasion and Promoted Apoptosis 4 Weeks After Treatment

Wound healing assays indicated that the width of scratches were gradually reduced (Figure 3A). Multiple comparisons of the 72 hour-scratch repair rates (Figure 3C) indicated that the rates in the experimental groups were significantly lower than in the control group (all  $P$  values were  $< .001$ ; 1-way ANOVA). The rate of the 6 Gy group was significantly lower than the 2 Gy ( $P = .002$ ) and 4 Gy groups ( $P = .003$ ).

As shown in Figure 3D, through multiple comparisons (1-way ANOVA), compared with the control group, the number of invading cells in the 2 Gy group exhibited a downward trend ( $P = .052$ ), but those in the 4 Gy and 6 Gy groups were significantly lower ( $P$  values were both  $< .05$ ). Statistical analyses also demonstrated that there were fewer invading cells in the 6 Gy group than in the 2 Gy group ( $P = .075$ ).

As shown in Figure 3B and E, multiple comparisons (1-way ANOVA) revealed that the apoptosis rates in the experimental groups were significantly higher than in the control group (all

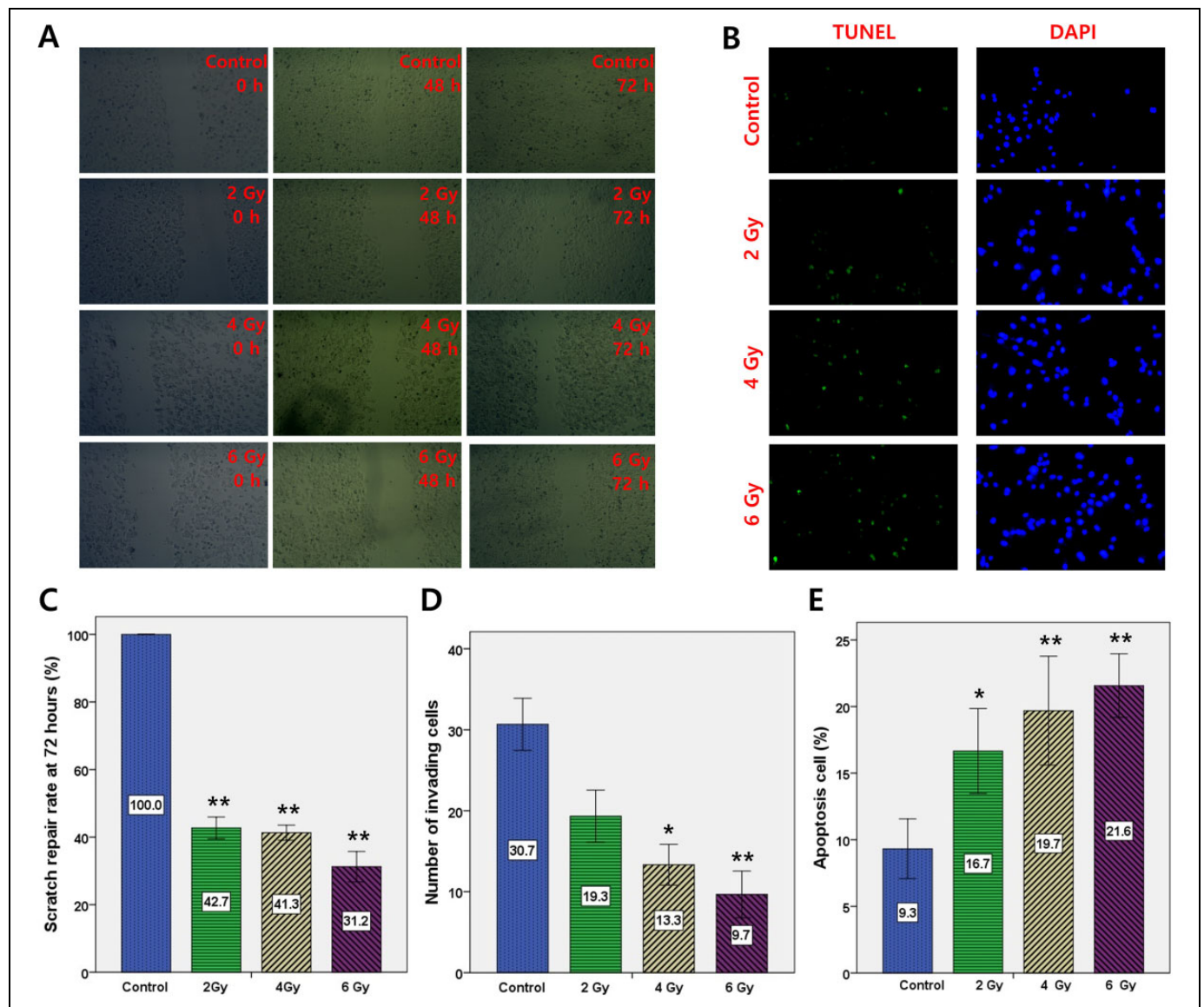


**Figure 3.** MCF-7 cell migration, invasion, and apoptosis assessments 4 weeks after single-dose irradiation by the Intrabeam device. Each experiment was repeated 3 times. A and C, Wound healing assays. Images of cells taken at 0, 48, and 72 hours after scratching in wound healing assays; quantitative analysis indicated that a single irradiation dose of 2, 4, or 6 Gy inhibited cell migration. D, Transwell assay indicated that a single irradiation dose of 4 or 6 Gy inhibited cell invasion. B and E, TUNEL apoptosis assay indicated that a single irradiation dose of 2, 4, or 6 Gy promoted cell apoptosis. Green: TUNEL-positive apoptotic cells; blue: nuclei stained with 4',6-diamidino-2-phenylindole (DAPI); magnification  $\times 100$ . C to E, Data are expressed as mean  $\pm$  SD; \* $P < .05$ , \*\* $P < .01$  (vs control group). SD indicates standard deviation; TUNEL, terminal deoxynucleotidyl transferase-mediated 2'-deoxyuridine 5'-triphosphate nick-end labeling.

$P$  values were  $<.05$ ), and the apoptosis rates in the 6 Gy group were generally higher than in the 2 Gy group ( $P = .086$ ).

## Discussion

Radiotherapy is a local treatment for cancer and affects the radiation target area by killing or inhibiting tumor cells. Radioactive rays include  $\alpha/\beta/\gamma$ /X-rays, electron beam, proton beam, and other proton beams, and ionizing radiation can generate biological effects including physical stage, chemical stage, and biological stage.<sup>14-16</sup> In some studies, Intrabeam IORT delivers

a single-radiation dose of 20 Gy to the tumor bed in breast-conserving surgery<sup>2</sup> or 16 Gy to the nipple-areola complex flap in nipple-sparing mastectomy.<sup>3</sup> Relative to the radiation energies of most EBRT devices ( $\sim$ MeV), the Intrabeam device only produces 50 kV X-rays. Here, we explored the functional changes in breast cancer cells after single-dose irradiation with the Intrabeam.

MCF-7 cells are invasive ductal carcinoma and luminal subtype cells.<sup>17-21</sup> Reportedly,<sup>22-24</sup> the luminal subtype accounts for approximately 60% of the 4 subtypes of breast cancer, and invasive ductal carcinoma is the major pathological type of

breast cancer. The effective radiation volume of IORT is much smaller than EBRT. Whether it is employed in breast-conserving surgery or nipple-sparing mastectomy, IORT is more appropriate for early- and middle-stage breast cancer during which tumor development is not fast. Compared to other commonly used invasive breast cancer cell strains (MDA-MB-231, MDA-MB-157, and T-47D), MCF-7 cells are weakly invasive.<sup>17,25</sup>

In our preliminary study of Intra-beam IORT for nipple-sparing mastectomy,<sup>3</sup> the prescribed radiation dose was 16 Gy. In the colony formation assays of the present study, 0 to 16 Gy were used as the radiation doses. We found that although few MCF-7 cells survived in the groups dosed with  $\geq 6$  Gy, no positive clone was identified. The results of our study (using a flat Intra-beam applicator) were consistent with those of Liu *et al*<sup>11</sup> and Marthinsen *et al*<sup>12</sup> using a spherical Intra-beam applicator. Moreover, we found that after MCF-7 cells received Intra-beam radiation at 2 to 6 Gy, most cells did not immediately die, some retained mitotic function, while a few could maintain mitosis for a long time. However, the proliferation speed was considerably reduced. After 2 to 3 weeks of culture and passage, the number of new dead cells in the experimental groups was significantly decreased. In the clinic, after radiation treatment with therapeutic doses, cancer cells resistant to radiotherapy still exist. Study of the response characteristics of these resistant cells could help in the selection of Intra-beam IORT combined with other therapeutic regimens. Thus, we explored short-term (24 hours) and long-term (about 4 weeks) changes in MCF-7 cells after Intra-beam radiation with single doses of 2 to 6 Gy.

In this study, at 24 hours after Intra-beam irradiation, the percentages of normal cells in the 4/6 Gy groups were reduced, and the percentages of cells in late apoptosis/necrosis in the experimental groups (2/4/6 Gy) were increased, but the percentages of early apoptotic cells in the experimental groups were similar to that in the control group. This may be because some radiation-sensitive cells immediately initiated apoptosis after Intra-beam radiation, and the ionizing radiation thermal effect generated by Intra-beam radiation promoted early-stage necrosis. Percentages of cells arrested in G<sub>1</sub> phase in the experimental groups were increased, but those in S phase and G<sub>2</sub> phase were decreased. This is consistent with the slow proliferation rates in the experimental groups after radiotherapy. We also found that, at day 2 and 3 after radiotherapy, the number of new dead cells gradually began to increase. This may be because some cells repaired themselves partially after Intra-beam radiation, finally leading to limited mitosis.

Radiotherapy leads to apoptosis and necrosis in MCF-7 cells and can also induce cell senescence and other biological changes.<sup>26-29</sup> In this study, we found that even at 4 weeks after single-dose irradiation with the Intra-beam, the proliferation rates of the cells in the experimental groups were slower than that in the control group. In the experimental groups, more granule-like substances could be observed in most of the cells, and more cells became swollen. In most studies, functional experiments with tumor cells were performed shortly after

radiotherapy.<sup>26,29-34</sup> However, after radiotherapy, the characteristics of sublethal tumor cells may change over time. In the study, at 4 weeks after single-dose irradiation with the Intra-beam, we found the following: (a) the migratory abilities of the experimental groups decreased in a dose-dependent manner; (b) invasiveness in the 4/6 Gy groups was lower than that in the control group; and (c) apoptosis rates of the experimental groups were all higher than that of the control group. Thus, we deduced that single-dose Intra-beam radiation might have a long-term effect on the inhibition of migration and invasion and promotion of apoptosis, with higher doses leading to more significant effects.

In conclusion, single-dose irradiation of 6 Gy using an Intra-beam device can effectively inhibit proliferation, migration, and invasion and promote apoptosis in MCF-7 cells with long-lasting effects.

### Authors' Note

Lingxiao Pan, Minghui Wan, and Wenbo Zheng, contributed equally. The current study was approved by the Ethics Committee of the First Affiliated Hospital of Guangzhou Medical University (registering order 201750).

### Declaration of Conflicting Interests

The author(s) declared no potential conflicts of interest with respect to the research, authorship, and/or publication of this article.

### Funding

The author(s) disclosed receipt of the following financial support for the research, authorship, and/or publication of this article: This study was supported by the Medical and Health Technology Project of Guangzhou Municipal Health Bureau (No. 20161A010078); the Health and Family Planning Technology Project of Guangzhou Municipal Health and Family Planning Bureau (No. 20181A011063).

### References

1. Siegel RL, Miller KD, Jemal A. Cancer statistics, 2018. *CA Cancer J Clin.* 2018;68(1):7-30.
2. Vaidya JS, Wenz F, Bulsara M, et al. Risk-adapted targeted intraoperative radiotherapy versus whole-breast radiotherapy for breast cancer: 5-year results for local control and overall survival from the TARGIT-A randomised trial. *Lancet.* 2014;383(9917):603-613.
3. Pan L, Zheng W, Ye X, et al. A novel approach of INTRABEAM intraoperative radiotherapy for nipple-sparing mastectomy with breast reconstruction. *Clin Breast Cancer.* 2014;14(6):435-441.
4. Vaidya JS, Tobias JS, Baum M, et al. Intraoperative radiotherapy for breast cancer. *Lancet Oncol.* 2004;5(3):165-173.
5. Giordano FA, Brehmer S, Abo-Madyan Y, et al. INTRAGO: intraoperative radiotherapy in glioblastoma multiforme—a phase I/II dose escalation study. *BMC Cancer.* 2014;14(1):992.
6. Guo S, Reddy CA, Kolar M, et al. Intraoperative radiation therapy with the photon radiosurgery system in locally advanced and recurrent rectal cancer: retrospective review of the Cleveland clinic experience. *Radiat Oncol.* 2012;7(1):110.
7. Rutkowski T, Wygoda A, Hutnik M, et al. Intraoperative radiotherapy (IORT) with low-energy photons as a boost in patients

- with early-stage oral cancer with the indications for postoperative radiotherapy: treatment feasibility and preliminary results. *Strahlenther Onkol.* 2010;186(9):496-501.
8. Cagnetta AB, Howard BM, Heaton HP, et al. Superficial X-ray in the treatment of basal and squamous cell carcinomas: a viable option in select patients. *J Am Acad Dermatol.* 2012;67(6):1235-1241.
  9. Wenz F, Schneider F, Neumaier C, et al. Kypho-IORT—a novel approach of intraoperative radiotherapy during kyphoplasty for vertebral metastases. *Radiat Oncol.* 2010;5(1):11.
  10. Belletti B, Vaidya JS, D'Andrea S, et al. Targeted intraoperative radiotherapy impairs the stimulation of breast cancer cell proliferation and invasion caused by surgical wounding. *Clin Cancer Res.* 2008;14(5):1325-1332.
  11. Liu Q, Schneider F, Ma L, et al. Relative Biologic Effectiveness (RBE) of 50 kV X-rays measured in a phantom for intraoperative tumor-bed irradiation. *Int J Radiat Oncol Biol Phys.* 2013;85(4):1127-1133.
  12. Marthinsen AB, Gisetstad R, Danielsen S, et al. Relative biological effectiveness of photon energies used in brachytherapy and intraoperative radiotherapy techniques for two breast cancer cell lines. *Acta Oncol.* 2010;49(8):1261-1268.
  13. Herskind C, Schalla S, Hahn EW, et al. Influence of different dose rates on cell recovery and RBE at different spatial positions during protracted conformal radiotherapy. *Radiat Prot Dosimetry.* 2006;122(1-4):498-505.
  14. Girdhani S, Sachs R, Hlatky L. Biological effects of proton radiation: an update. *Radiat Prot Dosimetry.* 2015;166(1-4):334-338.
  15. Swartz HM, Williams BB, Flood AB. Overview of the principles and practice of biodosimetry. *Radiat Environ Biophys.* 2014;53(2):221-232.
  16. Georgakilas AG, Pavlopoulou A, Louka M, et al. Emerging molecular networks common in ionizing radiation, immune and inflammatory responses by employing bioinformatics approaches. *Cancer Lett.* 2015;368(2):164-172.
  17. Neve RM, Chin K, Fridlyand J, et al. A collection of breast cancer cell lines for the study of functionally distinct cancer subtypes. *Cancer Cell.* 2006;10(6):515-527.
  18. Riaz M, van Jaarsveld MT, Hollestelle A, et al. miRNA expression profiling of 51 human breast cancer cell lines reveals subtype and driver mutation-specific miRNAs. *Breast Cancer Res.* 2013;15(2):R33.
  19. Hollestelle A, Nagel JH, Smid M, et al. Distinct gene mutation profiles among luminal-type and basal-type breast cancer cell lines. *Breast Cancer Res Treat.* 2010;121(1):53-64.
  20. Kao J, Salari K, Bocanegra M, et al. Molecular profiling of breast cancer cell lines defines relevant tumor models and provides a source for cancer gene discovery. *PLoS One.* 2009;4(7):e6146.
  21. Lacroix M, Leclercq G. Relevance of breast cancer cell lines as models for breast tumours: an update. *Breast Cancer Res Treat.* 2004;83(3):249-289.
  22. Dai X, Li T, Bai Z, et al. Breast cancer intrinsic subtype classification, clinical use and future trends. *Am J Cancer Res.* 2015;5(10):2929-2943.
  23. O'Brien KM, Cole SR, Tse CK, et al. Intrinsic breast tumor subtypes, race, and long-term survival in the Carolina Breast Cancer Study. *Clin Cancer Res.* 2010;16(24):6100-6110.
  24. Brenton JD, Carey LA, Ahmed AA, et al. Molecular classification and molecular forecasting of breast cancer: ready for clinical application? *J Clin Oncol.* 2005;23(29):7350-7360.
  25. Dai X, Cheng H, Bai Z, Li J, et al. Breast cancer cell line classification and its relevance with breast tumor subtyping. *J Cancer.* 2017;8(16):3131-3141.
  26. Huang YH, Yang PM, Chuah QY, et al. Autophagy promotes radiation-induced senescence but inhibits bystander effects in human breast cancer cells. *Autophagy.* 2014;10(7):1212-1228.
  27. Yu YC, Yang PM, Chuah QY, et al. Radiation-induced senescence in securin-deficient cancer cells promotes cell invasion involving the IL-6/STAT3 and PDGF-BB/PDGFR pathways. *Sci Rep.* 2013;3(4):1675.
  28. Jones KR, Elmore LW, Jackson-Cook C, et al. p53-Dependent accelerated senescence induced by ionizing radiation in breast tumour cells. *Int J Radiat Biol.* 2005;81(6):445-458.
  29. Li D, Ilnytsky Y, Kovalchuk A, et al. Crucial role for early growth response-1 in the transcriptional regulation of miR-20b in breast cancer. *Oncotarget.* 2013;4(9):1373-1387.
  30. Yu L, Yang Y, Hou J, et al. MicroRNA-144 affects radiotherapy sensitivity by promoting proliferation, migration and invasion of breast cancer cells. *Oncol Rep.* 2015;34(4):1845-1852.
  31. Li Q, Liu J, Meng X, Li J, et al. MicroRNA-454 may function as an oncogene via targeting AKT in triple negative breast cancer. *J Biol Res (Thessalon).* 2017;24(1):10.
  32. Croker AK, Rodriguez-Torres M, Xia Y, et al. Differential functional roles of ALDH1A1 and ALDH1A3 in mediating metastatic behavior and therapy resistance of human breast cancer cells. *Int J Mol Sci.* 2017;18(10):2039.
  33. Goode GD, Ballard BR, Manning HC, et al. Knockdown of aberrantly upregulated aryl hydrocarbon receptor reduces tumor growth and metastasis of MDA-MB-231 human breast cancer cell line. *Int J Cancer.* 2013;133(12):2769-2780.
  34. Körner C, Keklikoglou I, Bender C, et al. MicroRNA-31 sensitizes human breast cells to apoptosis by direct targeting of protein kinase C epsilon (PKCepsilon). *J Biol Chem.* 2013;288(12):8750-8761.